J. Serb. Chem. Soc. 72 (3) 275–287 (2007)
JSCS–3557

UDC 621.359.3+667.632.046:669.295
Original scientific paper

Electrophoretic deposition and thermal treatment of boehmite coatings on titanium

MARIJA S. DJOŠIĆ[1#], VESNA B. MIŠKOVIĆ-STANKOVIĆ[2*#] and VLADIMIR V. SRDIĆ[3,#]

[1]Institute for Technology of Nuclear and Other Mineral Raw Materials, Franše d'Eperea 86, 11000 Belgrade, [2]Faculty of Technology and Metallurgy, University of Belgrade, Karnegijeva 4, P. O. Box 3503, 11120 Belgrade and [3]Department of Materials Engineering, Faculty of Technology, University of Novi Sad, Bulevar Cara Lazara 1, 21000 Novi Sad, Serbia (e-mail: vesna@tmf.bg.ac.yu)

(Received 27 March, revised 29 June 2006)

Abstract: An aqueous boehmite sol was prepared by the peptization of $Al(OH)_3$. The electrophoretic deposition of boehmite coatings on titanium from the aqueous sol was performed at a constant voltage (from 1.0 to 10 V) and for a constant deposition time (from 10 to 30 min). Increasing the applied voltage and deposition time increased the mass of the boehmite coating. It was shown that boehmite coatings of maximum thickness, low porosity and good adhesion can be formed at lower deposition voltages and longer deposition times. The boehmite powder, obtained by drying the prepared aqueous sol, and the boehmite coatings were thermally treated at 1000 °C and 1300 °C with a holding period of 1 h at the maximum temperature. X-Ray diffraction analysis of the thermally treated samples confirmed the existence of γ-Al_2O_3 and α-Al_2O_3 phases, respectively, while scanning electron microscopy revealed the graininess of the structure of the α-Al_2O_3 coatings treated at 1300 °C, indicating a significantly lower sintering temperature of the boehmite coating obtained by electrophoretic deposition.

Keywords: boehmite sol, electrophoretic deposition, boehmite coating, titanium, thermal treatment.

INTRODUCTION

Electrophoretic deposition is gaining increasing attention both in science and industry,[1] due to novel application in the processing of advanced ceramic materials and ceramic coatings. Electrophoretic deposition has become very interesting because this method allows the formation of thin films or multilayer films of controlled thickness, enabling the formation of films on substrates of complex geometry.

Electrophoretic deposition is achieved *via* the motion of charged particles dispersed in a liquid towards an electrode under an applied electric field (electrophoresis),

* Corresponding author.

Serbian Chemical Society active member.

doi: 10.2298/JSC0703275D

with deposit formation occuring by particle coagulation. Using electrophoretic deposition it is possible to obtain glass–ceramic coating materials,[2] organoceramic materials,[3] composite materials,[4,5] ceramic films[6–9] and solid oxide fuel cells.[10,11] Electrophoretic phenomena have been investigated both in non-aqueous[12–14] and in aqueous media.[6,15–17] Non-aqueous media have much better performances compared to aqueous media (*e.g.* low viscosity), but environmental problems arise with the use of organic media. Accordingly, electrophoretic deposition should be performed from an aqueous solution whenever possible. The use of sol–gel routes in ceramic processing has many advantages, such as greater purity, higher homogeneity and ultrafine grain size distribution, in comparison to conventional powder-based processing techniques. Moreover, as the sol contains very sinter-active ceramic particles on a nanometer scale, the sintering temperatures can be lowered by several hundred degrees.[18]

The aim of this work was to investigate the effect of deposition parameters, *e.g.* applied voltage and deposition time on the mass and morphology of boehmite coatings on titanium, as well as the phase transformation in boehmite powder and coatings during the thermal treatment. A Ti substrate was chosen for the electrodeposition of boehmite coatings due to its thermal stability, with the aim of determining the sintering temperature of the boehmite deposits. Namely, it is well known that the deposition of ceramic particles from a sol leads to a significantly lower sintering temperature of the ceramic coating compared to coatings deposited from suspension.

EXPERIMENTAL

Preparation of the aqueous boehmite sol

The boehmite sol was prepared by the peptization of freshly precipitated $Al(OH)_3$, obtained by the addition of NH_4OH to an aqueous solution of $AlCl_3 \cdot 6H_2O$ (Merck, p. a.) at 80 °C up to pH 7– 8. The precipitate was then washed with hot water until a negative reaction of Cl^- ions with $AgNO_3$ was observed. $Al(OH)_3$ was suspended in distilled water and the appropriate amount of concentrated HNO_3 acid (Merck, p. a.) was added at a mole $n(HNO_3)/n(Al(OH)_3$ ratio of 0.1. The sol was prepared in a three-necked flask under reflux at 100 °C for 48 h. The pH of the prepared sol was 3.82.

Characterization of boehmite powder

Boehmite powder was obtained by drying the sol at 90 °C for 48 h. The solid phase content, determined gravimetrically, was 1.76 wt.%.

The phase composition and structure of the boehmite powder were determined by X-ray diffraction (XRD) analysis using a Philips PW 1710 difractometer with CuK_α radiation (λ = 0.154176 nm). The diffraction intensity was measured by the scanning technique in the 2θ range of 4 – 70° with 0.02° steps for 0.25 s per point.

The specific surface area of the solid phase was determined by the single point BET method using a Strohlein area meter.

Electrophoretic deposition of boehmite coatings on titanium from the aqueous sol

A three-electrode cell arrangement was used for the cathodic electrodeposition. The working electrode was a titanium plate (10 mm x 15 mm x 0.89 mm, Alfa Aesar, Johnson Matthew Co.). The two counter electrodes were platinum panels, placed parallel to the working electrode at a distance of 1.5 cm. The titanium plates were degreased in hot dilute hydrochloride acid solution (1:1) for 15 min and rinsed with distilled water.

The boehmite coatings were deposited on the titanium from the aqueous boehmite sol using the constant voltage method. The experiments were performed at different values of the constant voltage ranging between 1.0 and 10 V, for various deposition times of 10–30 min at room temperature.

The mass of the boehmite deposit was determined by weighing the cathode before and after deposition.

Characterization of the boehmite coatings on titanium

The boehmite coatings electrodeposited on titanium at 4.0 V and for a deposition time of 30 min were characterized by XRD, thermogravimetry (TG) and scanning electron microscopy (SEM).

XRD Analysis of the boehmite coatings dried at room temperature and the coatings sintered in air at 1000 °C and 1300 °C for 1 h, was performed under the same conditions as employed for boehmite powder.

TG Analysis of the boehmite coatings dried at room temperature in air was carried out under a nitrogen atmosphere (flow rate 30 cm^3 min^{-1}), using a Perkin–Elmer TGS-2 at a heating rate of 10 °C min^{-1} in the temperature range from 23 to 600 °C.

The microstructure of the boehmite coatings dried at room temperature in air and the coatings sintered in air at 1000 °C and 1300 °C for 1 h was examined by SEM using a Jeol JSM 6460 LV instrument, after vapor deposition of a conductive gold layer on the surface of the boehmite deposit.

RESULTS AND DISCUSSION

Characterization of boehmite powder

The XRD patterns of the boehmite powder and a boehmite coating are represented in Fig. 1. It may be seen that all the peaks of the boehmite powder corre-

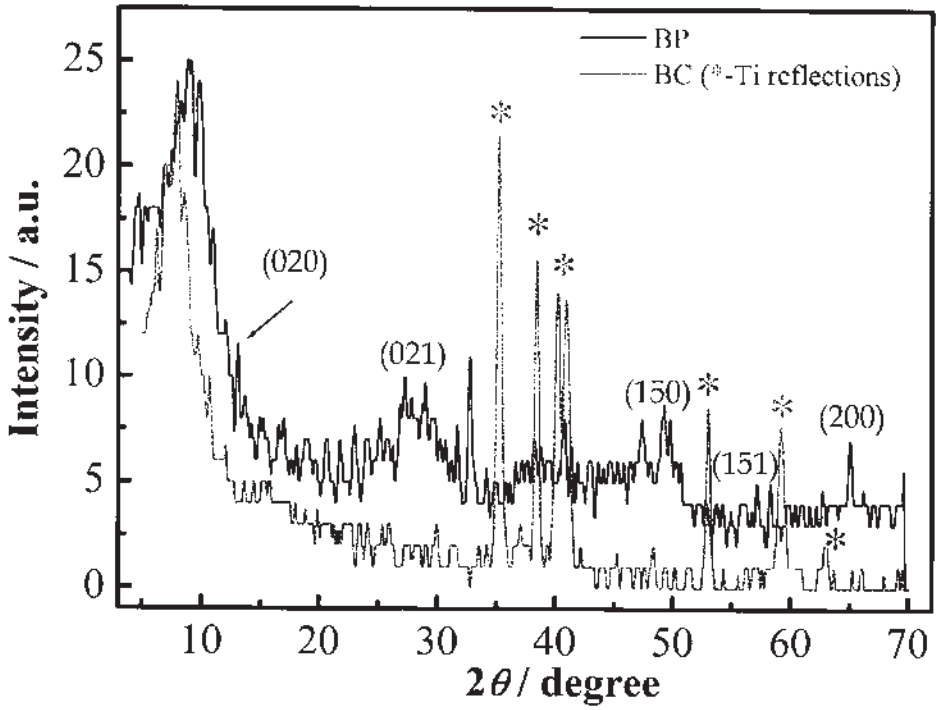

Fig. 1. XRD Patterns of the boehmite powder (BP) and boehmite coating (BC) dried at room temperature in air.

spond to the pseudoboehmite phase, except the one at the 2θ angle of 10°, which corresponds to scarboit ($Al_2(OH)_6 \cdot 6H_2O$). This peak probably originates from the $Al(OH)_3$, which remained as a residue after peptization with HNO_3.

According to the literature,[19,20] on the basis of the position of the (020) plane, the *d*-spacing lies between d_1-spacing (0.61 nm) and d_2-spacing (0.67 nm), which corresponds to boehmite and pseudoboehmite, respectively. From the peak position for the (020) plane in Fig. 1, the *d*-spacing was calculated to be 0.674 nm, which corresponds to the pseudoboehmite phase. Fig. 1 shows that the peaks are not sharp, which confirmed the pseudoboehmite phase, because it is well known that pseudoboehmite has lower crystallinity compared to boehmite.[21] The IR spectrum of boehmite powder also shows[22] the characteristic bands for the pseudoboehmite structure. The XRD pattern of the boehmite coating shows only the peak of Ti (which corresponds to the substrate), due to the small film thickness.

The specific surface area of boehmite powder, determined by the single point BET method, was calculated to be 220 $m^2\ g^{-1}$.

The effect of applied voltage and deposition time on the boehmite deposit mass

The necessary conditions which provide for a successful electrophoretic deposition are a stable suspension/sol, in which the particles have a high zeta potential, while the ionic conductivity of the suspension is kept at a low value.[23]

In the case of boehmite particles, the adsorption and desorption processes can be represented as follows:[24]

$$>AlOH + H^+ \rightleftarrows > AlOH_2^+ \qquad (pH < pH_{pzc}) \tag{1}$$

$$>AlOH + OH^- \rightleftarrows > AlOH^- + H_2O \qquad (pH > pH_{pzc}) \tag{2}$$

The pH of the prepared boehmite aqueous sol was 3.82, suggesting that the boehmite particles were positively charged (the pH at the point of zero charge, pH_{pzc} lies between 6.3 and 8.4[25]).

The electrophoretic deposition of boehmite particles occurs in several steps and is discussed in the literature.[6,15,22,26] The rate of migration which the particles can achieve, ν, is given by the Equation:

$$\nu = zE/6\pi\eta r \tag{3}$$

whre E is the applied electric field, η the suspension viscosity, r the particle radius and z the particle charge, indicating a linear dependence of the migration rate on the applied electric field. When an ion reaches the cathode, it discharges. As the particle is sufficiently close to the cathode, attractive forces dominate and coagulation/deposition occurs.

At voltages higher than approximately 2.0 V, hydrogen and oxygen evolve at the cathode and anode, respectively, due to the electrolytic decomposition of water:

$$\text{Cathode: } 2H^+ + 2e^- \rightarrow H_2 \text{ (pH 1–7)} \quad (4)$$

$$\text{or: } 2H_2O + 2e^- \rightarrow H_2 + 2OH^- \text{ (pH 7–14)} \quad (5)$$

$$\text{Anode: } 2H_2O \rightarrow 4H^+ + O_2 + 4e^- \text{ (pH 1–7)} \quad (6)$$

$$\text{or: } 4OH^- \rightarrow O_2 + 2H_2O + 4e^- \text{ (pH 7–14)} \quad (7)$$

During electrodeposition, the hydrogen bubbles evolve on the cathode, through the formed boehmite film. In addition, some hydrogen bubbles may remain trapped between the deposited sol particles, resulting, in both cases, in film porosity.[25] Indeed, the dependence of the deposition current density on the deposition time at a constant applied voltage,[22] corresponded to the deposition of porous films.[28,29]

The mass of the boehmite deposit, *m*, as a function of the applied deposition voltage, *U*, for different deposition times is shown in Fig. 2.

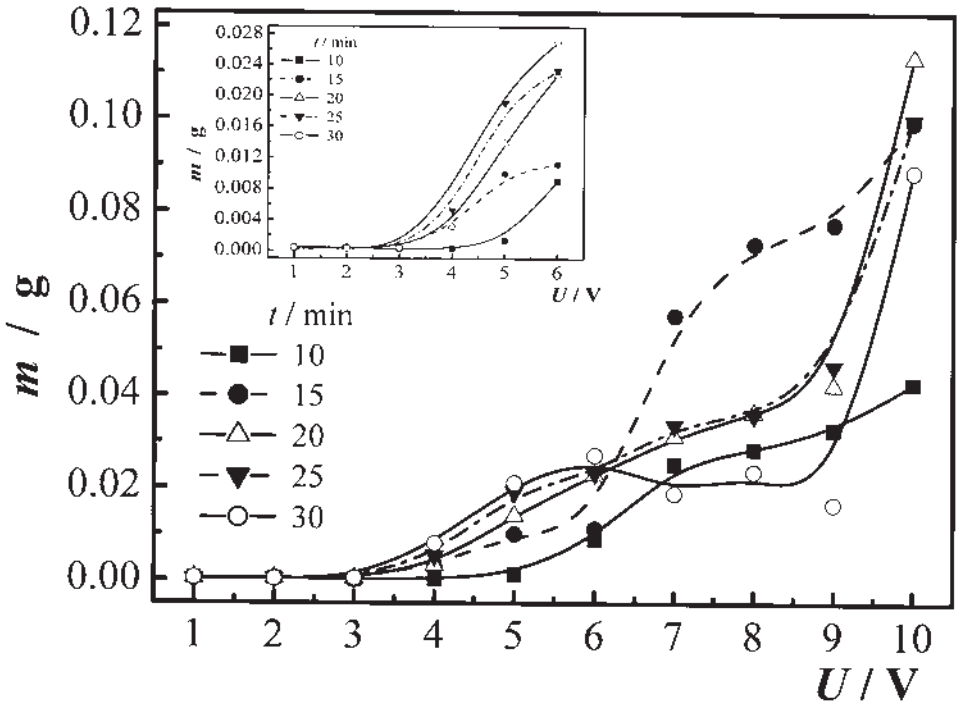

Fig. 2. Dependence of the mass of the boehmite deposit on the applied voltage for different deposition times, inset: *m, vs. U* curves at voltages up to 6.0 V.

With increasing applied voltage and deposition time, the mass of the boehmite deposit increased. According to Eq. (3), increasing the applied voltage increases the rate of particle migration and, consequently, the mass of the boehmite deposit. The rate of hydrogen evolution, as an undesirable process, also increases with in-

creasing applied voltage. At lower applied voltages, up to 3.0 V, the mass of the boehmite deposit was too small and neither the deposition time, nor the deposition voltage, influenced the process (inset in Fig. 2). A possible explanation is that the applied electric field is not sufficiently strong and that the rate of colloidal particle migration is too slow. At the same time, the applied voltage is insufficient to cause a destabilization of the boehmite sol near the electrode.

Increasing in the applied voltage from 3.0 to 6.0 V, for all deposition times, increases the mass of the boehmite deposit (inset in Fig. 2). Also, the rate of hydrogen evolution increases at applied voltages greater than 3.0 V, hence the amount of evolved hydrogen is larger, causing a greater porosity and cracks in the boehmite deposit during subsequent drying at room temperature. Poor adhesion of the boehmite deposit was observed at applied voltages higher than 4.0 V, although the mass of the boehmite deposit increased.

A decrease in the mass of the boehmite deposit was observed at voltages higher than 6.0 V for a deposition time of 30 min. This behavior can be explained by a larger amount of hydrogen evolved at the cathode at higher voltages and for longer deposition times, and, additionally, by poor adhesion of the boehmite coating.

The effect of deposition time on the mass of the boehmite deposit at different applied voltages is also shown in Fig. 2. At lower applied voltages, up to 3.0 V, an increase in the deposition time does not influence the mass of the boehmite deposit. At applied voltages from 3.0 V to 6.0 V, increasing the deposition time increases the mass of boehmite deposit due to more particles reaching the cathode. At voltages higher than 6.0 V, the mass of the boehmite deposit achieves a maximum and then decreases with increasing deposition time due to the larger amount of evolved hydrogen, which accumulates on the cathode and forms more pores in the deposited film.

Thus, it may be concluded that the optimal voltage for the boehmite deposition of a coating is 4.0 V, because it is the highest voltage at which a film of low porosity and good adhesion can be formed on titanium. On the other hand, the optimal deposition time is 30 min, since increasing the deposition time increases the mass of the boehmite deposit. Consequently, boehmite coatings of maximum thickness, low porosity and good adhesion were formed at longer deposition times and at lower deposition voltages. A coating electrodeposited at 4.0 V for a deposition time of 30 min was chosen for further thermal treatment at 1000 and 1300 °C, with a holding period of 1 h at the maximum temperature.

Thermogravimetric analysis of the boehmite coatings

The mass loss and temperatures associated with phase transformation were determined by thermogravimetry. The TG curve of the boehmite coating (U = 4.0 V, t = 30 min, dried at room temperature) obtained in the temperature range between 23 and 600 °C is shown in Fig. 3a, while Fig. 3b represents the differential TG (DTG) curve.

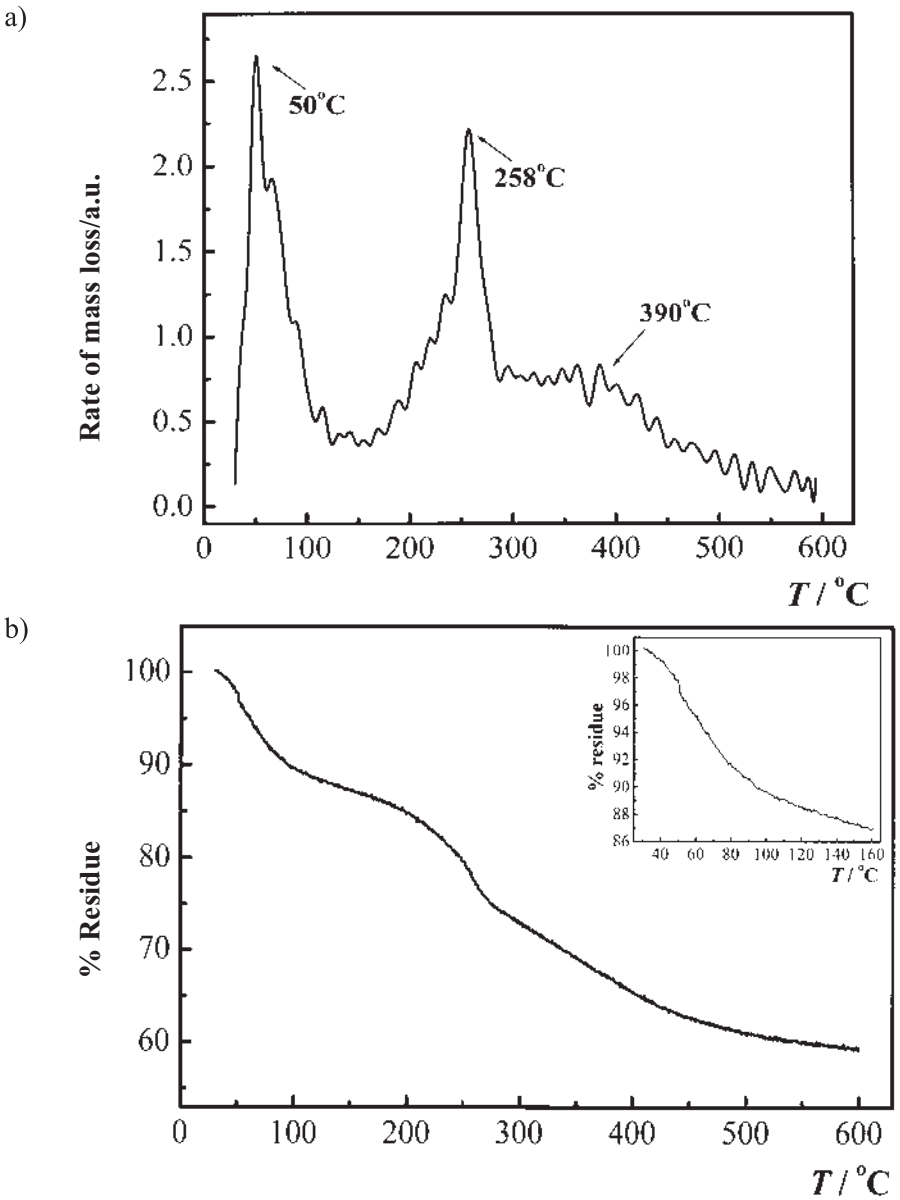

Fig. 3. (a) TG curve and (b) differential TG (DTG) curve of the boehmite coating (U = 4.0 V, t = 30 min, dried at room temperature in air), inset: TG Curve between 23 and 160 °C.

The TG curve of boehmite coating exhibited three characteristic mass loss stages. The first stage was observed from 23 °C to 160 °C (inset in Fig. 3b), with a sharp peak at 50 °C in the DTG curve (Fig. 3b). This stage corresponds to the desorption of water molecules adsorbed on the surface of the crystallites. It can be seen from the inset in Fig. 3b that water desorption occurs gradually. The mass loss in this stage in the initial

pseudoboehmite was calculated to be 13 wt. %. This is in accordance with data from the literature,[30] which showed that the mass loss in pseudoboehmite is higher than the mass loss in boehmite (about 1 wt. % in boehmite) due to the smaller crystallite size and thus a higher surface area avaliable for water adsorption. The observed mass loss can be explained by the boehmite structure. Namely, boehmite crystallites are made of doubled layers of octahedra sharing edges along the *a* axis and vertexes along the *c* axis, with an aluminium atom near their center and two hydroxyl groups and four oxygen atoms in their vertexes.[30,31] The octahedra in the doubled layers interact strongly with each other, hence, the interaction within a doubled layer is strong. However, betwen the doubled layers the interaction is weak, due to hydrogen bonds. Therefore, a boehmite crystallite ends in the interface between two doubled layers, thus producing surfaces that are full of hydroxyl groups. The crystallite surfaces perpendicular to the doubled layers have oxygen atoms in low coordination. These oxygen atoms can easily react with hydroxyl groups and hydrogen ions from their environment, thus allowing these surfaces to become fully covered by hydroxyl groups. Due to the smaller crystallite size in pseudoboehmite, the number of these low coordination oxygen sites increases, thus allowing more water molecules to be adsorbed. Thus the first peak in the DTG curve, located at 50 °C (Fig. 3b), corresponds to the desorption of water molecules from the boehmite surface.

The second stage of the mass loss on the TG curve was observed between 160 and 450 °C (Fig. 3a), which corresponds to the transition of boehmite into γ-Al_2O_3. Two peaks in the DTG curve were observed in the temperature interval: a sharp peak at 258 °C and broad peak at 390 °C (Fig. 3b). The peak at 258 °C and a mass loss of 11 wt.% between 50 and 258 °C, calculated from the TG curve, indicate the transformation of pseudoboehmite ($Al_2O_3 \cdot nH_2O$, where $1 < n < 2.5$)[32–35] into boehmite ($Al_2O_3 \cdot H_2O$)[30,35] and corresponds to 0.41 mol H_2O per mol boehmite. Consequently, the formula of the starting psuedoboehmite was calculated to be $AlOOH \cdot 0.41H_2O$ or $Al_2O_3 \cdot 1.82H_2O$. The excess water in pseudoboehmite is not surface, but interlayer water.[36] The mass loss of 15 wt.% between 258 and 390 °C, calculated from the TG curve (Fig. 3a), is associated with further boehmite transformation to γ-Al_2O_3 according to the Equation:

$$2AlOOH \rightarrow \gamma\text{-}Al_2O_3 + H_2O \quad (8)$$

and it corresponds to the theoretical mass loss of 15 wt.%.[37] The second, wide peak at 390 °C (DTG curve, Fig. 3b) corresponds to the transition from boehmite into γ-Al_2O_3, which occurs through partial dehydroxylation as a consequence of broken hydrogen bonds between the double layers in the boehmite crystallites.[30,31] The total mass loss of 26 wt.% in the second stage of the TG curve between 50 and 450 °C confirms the transformation from pseudoboehmite to γ-Al_2O_3.

The third stage of negligible mass loss at temperatures above 450 °C (Fig. 3a) corresponds to the transformation of γ-Al_2O_3 into the most stable α-Al_2O_3, *via* a sequence of transitional aluminas $\gamma \rightarrow \delta \rightarrow \theta \rightarrow \alpha$-$Al_2O_3$. This transition is a conse-

quence of the continuous and gradual loss of residual hydroxyl groups[37] and involves a reorganization of the oxygen into a denser, hexagonal closely packed configuration by nucleation and growth.[32,35]

The same results of phase transformations and calculated values of mass loss of the three characteristic mass loss stages, as well as the calculated formula of the starting pseudoboehmite, were obtained from thermogravimetry of boehmite powder,[22] indicating the same structure of the boehmite coating and boehmite powder, with no effect of the substrate on the structure of the boehmite coating.

Characterization of thermaly treated boehmite powder and coatings

The transformation of boehmite into the most stable α-Al_2O_3 phase occurs *via* a sequence of transitional aluminas $\gamma \rightarrow \delta \rightarrow \theta \rightarrow \alpha$-$Al_2O_3$ when their crystallites are completely dehydroxylated.

The XRD patterns of the boehmite powder and boehmite coating, both treated at 1000 °C for 1 h, are presented in Fig. 4. It may be seen that all the peaks for the treated boehmite powder, which are not sharp, correspond to γ-Al_2O_3, suggesting the begining of the crystallization process. The XRD pattern of the treated boehmite coating shows only the peaks of TiO_2 (which corresponds to the oxidized substrate) due to the small thickness of the film.

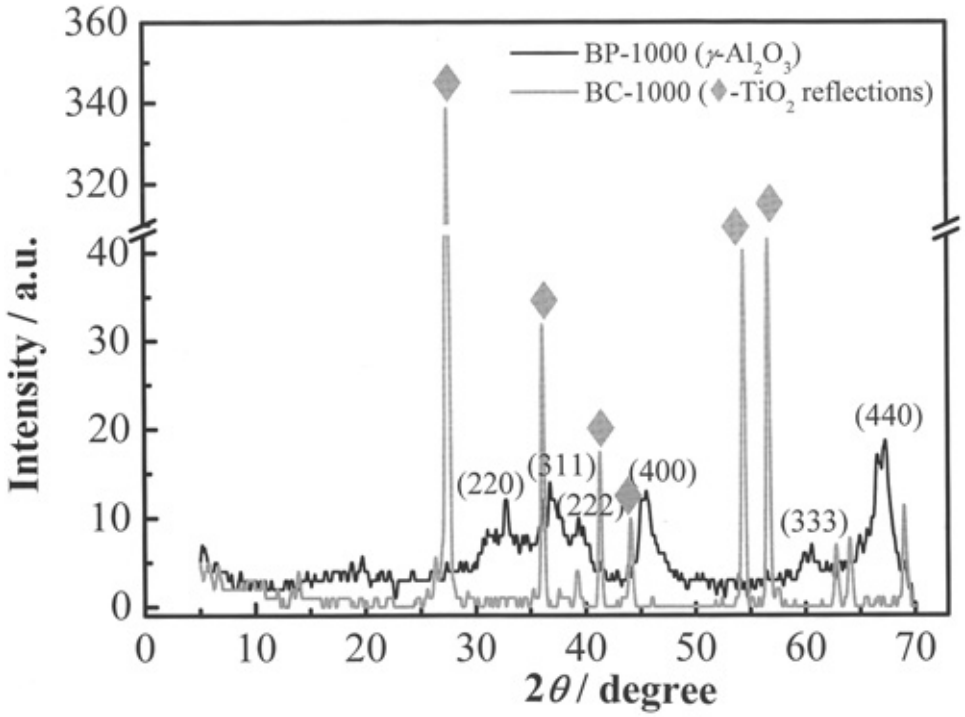

Fig. 4. XRD Patterns of the boehmite powder (BP-1000) and boehmite coating (BC-1000) (U = 4.0 V, t = 30 min) thermally treated at 1000 °C.

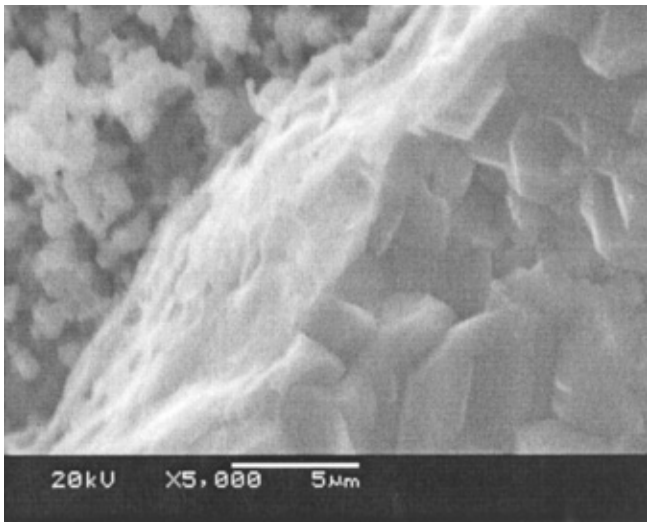

Fig. 5. SEM Micrograph of the boehmite coating (U = 4.0 V, t = 30 min) sintered at 1000 °C (magnification 5000x).

The SEM micrograph (Fig. 5) shows the boehmite coating treated at 1000 °C for 1 h. According to the analysis of the XRD pattern of the boehmite powder treated at the same manner (Fig. 4), it could be concluded that the boehmite coating is also γ-alumina, bearing in mind the results obtained from the TG of both the powder and the coating.

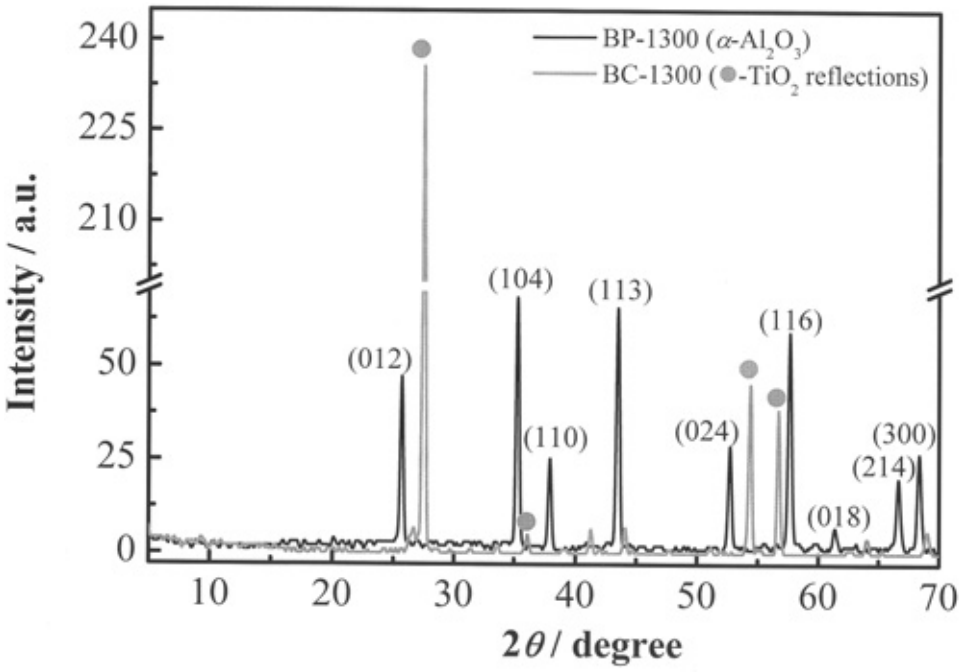

Fig. 6. XRD Patterns of the boehmite powder (BP-1300) and boehmite coating (BC-1300) (U = 4.0 V, t = 30 min) thermally treated at 1300 °C.

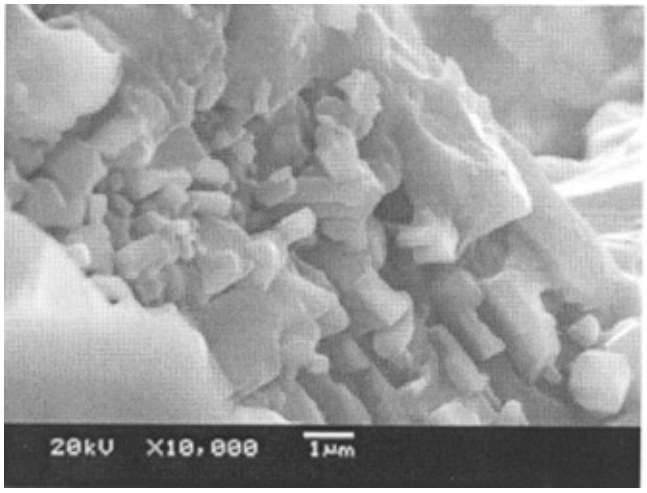

Fig. 7. SEM Micrograph of the boehmtie coating (U = 4.0 V, t = 30 min) sintered at 1300 °C (magnification 10000x).

The XRD patterns of the boehmite powder and boehmite coating, both treated at 1300 °C for 1 h, are presented in Fig. 6. It may be seen that all the peaks for the treated boehmite powder, which are sharp, correspond to the α-Al_2O_3, suggesting a high crystallinity of the corundum crystalites. The XRD pattern of the treated boehmite coating again shows only the peaks of TiO_2 (which corresponds to the oxidized substrate) again due to the small thickness of the film.

Comparing XRD patterns of the boehmite powder dried at room temperature, with those of the samples treated at 1000 °C and 1300 °C (Figs. 1, 4 and 6, respectively) it can be observed that increasing the temperature of thermal treatment (from room temperature to 1300 °C), increases the sharpness of the peaks, suggesting an increase in the crystallinity of the samples thermally treated at the higher temperatures.

The SEM micrograph of the boehmite coating treated at 1300 °C for 1 h (Fig. 7) shows the graininess of the coating of α-Al_2O_3, which is in accordance with the XRD data of boehmite powder treated at the same temperature (Fig. 6), bearing also in mind the results obtained from TG of both the powder and the coating. This indicates that the sintering temperature of the boehmite coating obtained by electrophoretic deposition from sol is lower compared to the sintering temperature (1600 °C) of boehmite coatings obtained by classical preparation methods.[38]

CONCLUSIONS

An aqueous boehmite sol was prepared by the peptization of $Al(OH)_3$ and characterized by XRD and BET. The pseudoboehmite phase was detected in the prepared aqueous sol by XRD analysis. On the basis of the peak position for the (020) plane, the d-spacing was calculated to be 0.674 nm.

The influence of the applied voltage and deposition time on the mass and morphology of the boehmite deposit on titanium was investigated. It was shown that

boehmite coatings of maximum thickness, low porosity and good adhesion can be formed at lower deposition voltages using longer deposition times.

The thermal properties of the boehmite coatings, *i.e.*, water desorption and phase transformation from pseudoboehmite to α-alumina, were analyzed by thermogravimetry. The starting formula of pseudoboehmite was calculated from these results to be $AlOOH\cdot 0.41H_2O$.

The coatings electrodeposited at 4.0 V for a deposition time of 30 min were treated at 1000 °C and 1300 °C. X-Ray diffraction and SEM analyses confirmed γ-Al_2O_3 and α-Al_2O_3, respectively, indicating a significantly lower sintering temperature of the boehmite coating obtained by electrophoretic deposition from the aqueous sol than by classical forming method.

Acknowledgements: This research was financed by the Ministry of Science and Environmental Protection, Serbia, contract number 142061.

ИЗВОД

ЕЛЕКТРОФОРЕТСКО ТАЛОЖЕЊЕ И СИНТЕРОВАЊЕ ПРЕВЛАКА БЕМИТА НА ТИТАНУ

МАРИЈА С. ЂОШИЋ[1], ВЕСНА Б. МИШКОВИЋ–СТАНКОВИЋ[2] и ВЛАДИМИР В. СРДИЋ[3]

[1]Институт за технологију нуклеарних и других минералних сировина, Франше д'Епереа 86, 11000 Београд, [2]Технолошко-металуршки факултет Универзитета у Београду, п. пр. 3503, 11120 Београд и [3]Технолошки факултет, Универзитет у Новом Саду, Булевар Цара Лазара 1, 21000 Нови Сад

Водени сол бемита је припремљен пептизацијом $Al(OH)_3$. Електрофоретско таложење превлака бемита из воденог сола вршено је при константном напону 1,0 до 10 V) и за константна времена таложења (10 до 30 min). Повећање напона и продужавање времена таложења доводи до пораста масе превлаке. Показано је да се превлаке највеће дебљине, мале порозности и добре адхезије могу формирати на нижим напонима и при дужим временима таложења. Резултати анализе дифракције X-зрака и скенирајуће електронске микроскопије су потврдили да су синтеровањем праха бемита и превлаке бемита на температурама од 1000 °C и 1300 °C добијени γ-алумијум-оксид и α-алуминијум-оксид, респективно. То указује на значајно снижење температуре синтеровања праха бемита и хомогене превлаке бемита добијене електрофоретским таложењем из сола.

(Primqeno 27. marta, revidirano 29. juna 2006)

REFERENCES

1. A. . Boccaccini, I. Zhitomirsky, *Current Opinion in Solid State and Materials Science* **6** (2002) 251
2. S. Data, *Bull. Mater. Sci.* **23** (2000) 125
3. I. Zhitomirsky, A. Petric, *Am. Ceram. Soc. Bull.* **80** (2001) 41
4. C. Kaya, F. Kaya, A. R. Boccaccini, *J. Mater. Sci.* **37** (2002) 4145
5. Z. Zhang, Y. Huang, Y. Jiang, *J. Am. Ceram. Soc.* **77** (1994) 1946
6. K. Simović, V. B. Mišković-Stanković, D. Kićević, P. Jovanović, *Colloids Surf. A: Physicochem. Eng. Aspects* **209** (2002) 47
7. M. Guglielmi, A. Licculli, S. Mazzarelli, *Ceram. Acta* **6** (1994) 19
8. M. Lazić, V. B. Mišković-Stanković, P. Jovanović, K. Simović, *Interceram* **51** (2001) 328

9. H. Nishimori, M. Tatsumisago, T. Minami, *J. Mater. Sci.* **31** (1996) 6529
10. C. Argirusis, T. Damjanović, G. Borchardt, *Key Eng. Mater.* **314** (2006) 101
11. C. Argirusis, T. Damjanović, G. Borchardt, *Mater. Sci. Forum* **453-454** (2004) 335
12. I. Zhitomirsky, L. Gal-Or, A. Kohn, H. W. Hennicke, *J. Mater. Sci.* **30** (1995) 5307
13. J. M. Park, S. I. Lee, K. W. Kim, D. J. Yoon, *J. Colloid Interface Sci.* **237** (2001) 80
14. E. de Beer, J. Duval, E. A. Meulankamp, *J. Colloid Interface Sci.* **222** (2000) 117
15. B. Ferrari, R. Morreno, *J. Eur. Ceram. Soc.* **17** (1997) 549
16. J. Y. Choudhary, H. S. Ray, K. N. Rai, *Trans. J. Br. Ceram. Soc.* **81** (1982) 189
17. R. Fischer, E. Fischer, G. de Portu, E. Roncari, *J. Mater. Sci. Lett*. **14** (1005) 25
18. A. R. Boccaccini, C. Kaya, *Ceram. Int.* **28** (2002) 893
19. R. Petrović, S. Milonjić, V. Jokanović, Lj. Kostić-Gvozdenović, I. Petrović-Prelević, Đ. Janaćković, *Powder. Techn.* **133** (2003) 185
20. H. Souza Santos, P. K. Kiohara, P. Souza Santos, *Mater. Res. Bull.* **31** (1996) 799
21. K. Okada, T. Ngashima, Y. Kameshima, A. Yasumori, T. Tsukada, *J. Colloid Interface Sci.* **253** (2002) 308
22. M. S. Đošić, V. B. Mišković-Stanković, Đ. T. Janaćković, Z. M. Kačarević-Popović, R. D. Petrović, *Colloids Surf. A: Physicochem. Eng. Aspects* **274** (2006) 185
23. O. O. Van der Biest, L. J. Vandeperre, *Annu. Rev. Mater. Sci.* **29** (1999) 327
24. M. Đ. Petković, S. K. Milonjić, V. T. Dondur, *Bull. Chem. Soc. Jpn.* **68** (1995) 2133
25. Ž. N. Todorović, S. K. Milonjić, V. T. Dondur, *Mater. Sci. Forum* **453-454** (2004) 361
26. P. Sarkar, P. S. Nicholson, *J. Am. Ceram. Soc.* **79** (1996) 1987
27. A. R. Boccaccini, H. Kern, H. . Kruger, P. A. Trusty, D. M. R. Taplin, *Proc. 43th International Scientific Colloquium,* Technical Univesity of Ilmenau, Ilmenau, Germany, 21–24 September 1998, p. 630
28. V. B. Mišković, M. D. Maksimović, *Surf. Technol.* **26** (1985) 353
29. P. E. Pierce, Z. Kovac, C. Higginbotham, *Ind. Eng. Chem. Prod. Res. Dev.* **17** (1978) 317
30. M. L. Guzman-Castillo, X. Bokhimi, A. Toledo-Antonio, J. Salmones-Blasquez, F. Hernandez-Beltran, *J. Phys. Chem. B* **105** (2001) 2099
31. X. Bokhimi, J. A. Toledo-Antonio, M. L. Guzman-Castillo, B. Mar-Mar, F. Hernandez – Beltran, J. Navarrete, *J. Solic State Chem.* **161** (2001) 319
32. J. Temuujin, T. Jadambaa, K. J. D. Mackenzie, P. Angerer, F. Porte, F. Riley, *Bul. Mater. Sci.* **23** (2000) 301
33. P. A. Buining, C. Pathmamanoharan, J. B. H. Jansen, H. N. W. Lekkerkerker, *J. Am. Ceram. Soc.* **74** (1991) 1303
34. E. Morgado, Jr. Y. L. Lam, L. F. Nazar, *J. Colloid Interface Sci.* **188** (1997) 257
35. S. Keysar, G. E. Shter, Y. Hazan, Y. Cohen, *Chem. Mater.* **9** (1997) 2464
36. J. M. Rousseaux, P. Weisbecker, H. Muhr, E. Plasari, *Ind. Eng. Chem. Res.* **41** (2002) 6059
37. T. Tsukada, H. Segawa, A. Yasumori, K. Okada, *J. Mater. Chem.* **9** (1999) 549
38. W. D. Kingery, H. K. Bowen, D. R. Uhlmann, *Introduction to Ceramics*, Wiley, New York, 1975.